Science of the Total Environment 747 (2020) 141266

Contents lists available at ScienceDirect

Science of the Total Environment

journal homepage: www.elsevier.com/locate/scitotenv

Evaluation of the Semi-Continuous OCEC analyzer performance with the EUSAAR2 protocol

A. Karanasiou [a,*], P. Panteliadis [b], N. Perez [a], M.C. Minguillón [a], M. Pandolfi [a], G. Titos [a,c], M. Viana [a], T. Moreno [a], X. Querol [a], A. Alastuey [a]

[a] Institute of Environmental Assessment and Water Research (IDAEA), Spanish Research Council (CSIC), Barcelona, Spain
[b] GGD, Department of Air Quality, Public Health Service Amsterdam, 1018WT, the Netherlands
[c] Department of Applied Physics, University of Granada, Granada 18071, Spain

HIGHLIGHTS

- We assessed the performance of EUSAAR2 protocol with the Semi-Continuous OCEC analyzer.
- Semi-Continuous OC, EC yielded very good agreement with offline OC, EC for denuded and undenuded samples.
- BC data were in very good agreement with Semi-Continuous EC concentrations.
- We detected split point shift and changes of PC due to the accumulation of refractory material.
- Thermograms should be carefully examined when dust events occur to consider interferences.

GRAPHICAL ABSTRACT

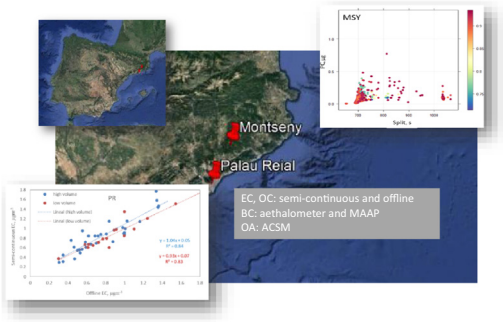

ARTICLE INFO

Article history:
Received 14 June 2020
Received in revised form 9 July 2020
Accepted 24 July 2020
Available online 27 July 2020

Editor: Pavlos Kassomenos

Keywords:
Elemental carbon
Organic carbon
Carbonaceous aerosol
Thermal-optical analysis

ABSTRACT

This work evaluates the applicability of the reference protocol EUSAAR2 in the Semi-Continuous OCEC analyzer under two environments, an urban background site influenced by traffic emissions and a regional background site. The comparison of the 24-h averaged OC and EC measurements of the Semi-Continuous analyzer with the OC and EC concentrations determined offline in $PM_{2.5}$ 24 h filters yielded very good agreement for both denuded and undenuded samples. In the urban background site, the regression for EC yielded a slope of 0.93 and 1.04 ($b = 0.07$ and 0.05, $R^2 = 0.83$ and 0.84), for denuded and undenuded samples respectively. The slopes of OC regressions were 0.99 ($b = -0.18$, $R2 = 0.81$) for the low volume and 0.93 ($b = 0.12$, $R^2 = 0.84$) for the high volume samples. In the regional background site, the slopes of the EC regression with the denuded and undenuded samples was 0.91 and 1.02 correspondingly ($b = 0$ and -0.03, $R^2 = 0.77$ and 0.89). The regression of OC had slopes close to 1; 1.03 for the high volume and 0.95 for the low volume sampler ($b = 0.08$ and 0.26, $R^2 = 0.78$ and 0.78). BC measurements obtained by an aethalometer and MAAP were in very good agreement with EC at both sampling sites. BC levels were consistently higher than EC (slope of the regression aethalometer BC vs EC slope $a = 1.2$, intercept $b = 0.19$, $R^2 = 0.79$, for the urban background site and $a = 1.9$, $b = -0.04$, $R2 = 0.94$, for the

Abbreviations: ACSM, Aerosol chemical speciation monitor; ACTRIS, European Research Infrastructure for the observation of Aerosol, Clouds and Trace Gases; BC, Black carbon; BrC, Brown carbon; CC, Carbonate carbon; CEN, European Committee for Standardization; CSN, Chemical Speciation Network; DRI, Desert Research Institute; EC, Elemental carbon; EUSAAR, European supersites for atmospheric aerosol research; GAW, Global atmosphere watch; IMPROVE, Interagency monitoring of protected visual environments; LOD, Limit of detection; MAAP, Multi-angle absorption photometer; MAC, Mass absorption cross section; OA, Organic aerosol; OC, Organic carbon; PC, Pyrolytic carbon; PM, Particulate matter; RIE, Relative ionization efficiency; SD, Standard deviation; SVOCs, Semi-volatile organic compounds; TC, Total carbon; TOA, Thermal-optical analysis; TOT, Thermal-optical transmittance; VOCs, Volatile organic compounds.

* Corresponding author.
E-mail address: angeliki.karanasiou@idaea.csic.es (A. Karanasiou).

https://doi.org/10.1016/j.scitotenv.2020.141266

African dust
Refractory material

regional site, slope MAAP BC vs EC a = 1.2, b = 0.06, R^2 = 0.94, for the urban background site and 1.7, b = −0.03, R^2 = 0.96, for the regional site). This confirms the need of using the site-specific mass absorption cross section (MAC) instead of the ones provided by manufacturers for the conversion of absorption units into BC mass concentration. BC data correlated very well with the optical EC obtained from the semi-continuous OCEC analyzer (a = 1.3, b = 0.16, R^2 = 0.80 for the urban background site and a = 1.7, b = 0.009, R^2 = 0.94 for the regional site, respectively). The comparison of OC concentrations by the Semi-Continuous Sunset analyzer with organic aerosol online measurements by ACSM showed strong correlations. The ratio OA/OC was 1.9 and 2.3 for the urban background and regional sites. The accumulation of refractory material on the filter, because of prolonged periods of sampling, caused a shift of the split point to the inert mode and changes on PC formation and evolution. Extreme dust outbreaks lead to the overestimation of OC due to the evolution of carbonate in the He mode. Generally, the Sunset Semi-Continuous OCEC analyzer with EUSAAR2 provided robust and consistent measurements with offline thermal-optical analysis.

1. Introduction

Carbonaceous aerosols have been drawn the attention of the research community because of their adverse effects on human health and climate (Bond et al., 2013; Janssen et al., 2011). They build up an important component of atmospheric particulate matter (PM) forming typically 20 to 50% of total aerosol mass in urban and regional background sites across Europe (Putaud et al., 2010). Particulate carbon (C) is usually classified into two major categories, organic carbon (OC) and elemental carbon (EC). OC stands for the C contained in thousands of individual compounds that can be of both primary and secondary origin, i.e. emitted directly into the atmosphere or formed into the atmosphere from volatile organic compounds (VOCs) (Jimenez et al., 2009). In contrast, EC is exclusively of primary origin and emitted by the incomplete combustion of carbon-based fuels, principally fossil fuels used in transportation, power generation, and industrial processes, and biomass used for residential heating and agricultural burns (Fuzzi et al., 2006).

Thermal-optical analysis (TOA) has been widely used for the determination of OC and EC in atmospheric aerosols. According to this method, the carbonaceous species are thermally desorbed firstly in an inert atmosphere (He) and then in an oxidizing atmosphere (mixture of He and O_2). Ideally, OC desorbs in the inert atmosphere while EC combusts in the oxidizing atmosphere at high temperature (Karanasiou et al., 2015). However, thermally unstable organic compounds might be pyrolytically converted into EC (char) when heated up in inert atmosphere. The formation of pyrolytic carbon (PC), which darkens the filter, is used to correct the measurement for charring, by continuously monitoring the transmittance or reflectance of the filter during the analysis. The point where the laser transmittance or reflectance reaches its initial value indicates that PC is completely evolved, and defines the split between OC and EC (Bae et al., 2004; Birch and Cary, 1996). The most commonly employed thermal protocols for the analysis of OC and EC in atmospheric aerosols are the IMPROVE (Chow et al., 1993), NIOSH-like protocols being modified versions of the Birch and Cary (1996) and Birch (1998) protocols, and the EUSAAR2 (Cavalli et al., 2010) protocol.

The Sunset OCEC and the DRI analyzer are commercially available instruments that use TOA for the offline determination of EC and OC deposited on filters. Both analyzers are capable to operate any thermal protocol either with transmittance or reflectance correction. In addition, a Semi-Continuous OCEC analyzer, developed by Sunset Laboratories, provides measurements of OC and EC on a customizable sampling time (usually varying from 1 to 3 h intervals) allowing for Semi-Continuous sampling with online analysis immediately after sample collection without requirement of offline sample treatment or laboratory analysis (Bae et al., 2004).

Precise determination and continuous monitoring of carbonaceous aerosols is essential for reducing uncertainty in climate change models (Kanakidou et al., 2005) and is important for long-term air quality assessment. The Air Quality Directive (2008/50/EC) requires the measurement of OC and EC in $PM_{2.5}$ in background sites with the objective of supporting air quality assessment and management. Nevertheless, EC and OC levels are not continuously measured in most of the environmental monitoring networks (Contini et al., 2018). To assist EU Member States meeting the requirements of the Air Quality Directive, the European Commission issued Mandate M/503 “Ambient air quality” for the development of “standards concerning automated measurements of particle matter in ambient air and the measurement of its chemical composition (OC and EC, inorganic components).” Consequently, the Working Group WG 35 of the European Committee for Standarization (CEN) elaborated a new standard for the measurement of airborne EC and OC in $PM_{2.5}$as no European standard previously existed (Karanasiou et al., 2015; Brown et al., 2017). The thermal-optical offline analysis of filter samples with transmittance correction (TOT) and the EUSAAR2 thermal protocol was adopted as the reference methodology for the determination of EC and OC in ambient $PM_{2.5}$ (EN16909:, 2017). This recently developed standard is likely to be used by all Member States as the reference method. In addition, the developed standard is expected to be extended to automated, (semi) real-time methods used to measure OC and EC such as the Sunset Semi-Continuous OCEC analyzer.

The field-deployable Sunset Semi-Continuous OCEC analyzer mostly uses NIOSH-like thermal protocols to determine OC, and EC at (semi) real-time (Brown et al., 2019; Bauer et al., 2009). An intercomparison study between the Semi-Continuous Sunset OCEC analyzer and the Sunset Lab OCEC analyzer demonstrated that the two analyzers yield well correlated and comparable results when a NIOSH-like protocol was used. The regression of OC measurements with the Sunset Lab OCEC analyzer vs. OC measured with the Semi-Continuous Sunset OCEC analyzer reached a correlation coefficient of 0.90, slope of 0.93 and a positive intercept of 0.94. The correlation of the results of EC measurements using these two analyzers had a poorer correlation (R^2 = 0.60) due to low levels of EC (compared to OC) but a regression slope of 0.95, and intercept b = 0.09 (Bae et al., 2004). Similarly, Snyder and Schauer (2007) found the Sunset Semi-Continuous measurements with a NIOSH-like protocol compared well with 24 h filter measurements (R^2 = 0.90, slope = 1.11 and b = 0.17 for EC). Recently, Brown et al. (2019) evaluated the utility of the Sunset Semi-Continuous OCEC analyzer with a NIOSH-like protocol and transmittance correction for charring in the Chemical Speciation Network (CSN) in the United States. The integrated measurements of the Sunset Semi-Continuous analyzer were compared with the results of the 24 h filter samples analyzed offline by the DRI C analyzer using the IMPROVE protocol with reflectance correction. Sunset OC fairly compared with the offline OC (R^2 = 0.67, slope = 0.67 and b = 0.77 μgm^{-3}). Sunset EC and offline EC did not compare as well (R^2 = 0.22, slope = 0.39 b = 0.56), in part because 26% of the hourly Sunset EC measurements were below the detection limit. We found only one study that deployed the EUSAAR2 protocol in the Sunset Semi-Continuous OCEC analyzer and

compared it with the offline TOT analysis (Malaguti et al., 2015), in a coastal site in central Mediterranean over a two months' period. Organic carbon 24 h offline measurements were 32.5% higher than those obtained with the Semi-Continuous analyzer.

This work evaluates the performance of the Semi-Continuous OCEC analyzer using the EUSAAR2 protocol as following the requirement for the networks of all EU Member States to measure EC and OC in $PM_{2.5}$ at background sites according to the Council Directive 2008/50/EC. We evaluate the applicability of the reference protocol to the online TOA method at two challenging environments, an urban background site influenced by traffic emissions and a regional background site. The application of the reference protocol to the Semi-Continuous OCEC analyzer and the comparison with offline TOA and with other methods, e.g. Black Carbon (BC) from absorption measurements can provide an insight on their comparability when examining the high-time resolution concentrations of carbonaceous aerosol. We further explore the performance of the Semi-Continuous analyzer with high concentrations of mineral dust and investigate the presence of a potential OCEC split point bias due to metal oxides accumulation caused by prolonged periods of sampling on the same filter.

2. Materials and methods

2.1. Sampling sites

The measurements took place at the urban background air quality monitoring super-site of Palau Reial (PR) located within the premises of IDAEA-CSIC in Barcelona, Spain (41° 23′14.28″N, 2°6′56.34″E, 77 m a.s.l) and at the Montseny (MSY) regional background super-site, located in a valley in the Montseny range, 40 km NNE of the Barcelona urban area and 25 km from the Mediterranean coast (41°46′45.63″N, 02°21′28.92″E, 720 m a.s.l), Fig. 1. Both sites belong to IDAEA-CSIC infrastructures and form part of the air quality monitoring network of the Department of Environment of the Autonomous Government of Catalonia. The MSY site is also integrated in to the Global Atmosphere Watch (GAW) and ACTRIS Networks. The PR site is highly influenced by vehicle emissions from the Diagonal Avenue located at 300 m with a traffic flow of around 100,000 cars/working day. The MSY site is a typical regional background site in a forested area affected by a large variety of other emission sources: natural sources contribution such as African dust and biogenic sources, marine aerosols, biomass burning, urban, traffic and industrial emissions from densely populated areas along the coastline and transboundary sources from the European continent (http://www.idaea.csic.es/egar/sites/).

2.2. Methodology

Measurements were conducted during two intensive sampling campaigns. A Semi-Continuous OCEC aerosol analyzer (Sunset Laboratory Inc.) equipped with a $PM_{2.5}$ cyclone at a flow rate of 8.0 l/min was installed at the urban background site (PR) from April 22 to September 26, 2016 and at the regional background site (MSY) from September 29, 2016 to March 1, 2017. The device was equipped with a C parallel-plate diffusion denuder to remove VOCs that can be adsorbed on quartz fibre filters and cause positive artefacts in the OC measurement (Viana et al., 2006). However, the use of the denuder may increase the magnitude of negative artefacts due to volatilization, since decreasing organic vapour pressures favours volatilization of organic carbon from particles already collected on the filter (Viana et al., 2006). Arhami et al. (2006) investigated the positive and negative sampling artefacts in the Sunset Semi-

Fig. 1. Locations of the Palau Reial and Montseny monitoring sites.

Continuous analyzer with and without a denuder. The positive artefact was found to be relatively large, more than 50% of measured OC, but it was practically eliminated when the denuder was used. The negative artefact was much smaller and may be neglected.

Ambient aerosols were collected on a quartz fibre filter (PALL) mounted in the central part of the oven, inside the instrument. After preliminary tests the time resolution was set at 4 h intervals (08:00, 12:00, 16:00, 20:00, and 24:00 local time) to reach accumulated EC and OC above the detection limits. Control calibrations by standard sucrose solution and test filters were performed every two weeks. Instrument blanks (0 min sampling) were measured once per day at 00:00 to check the stability of the instrument. The quartz fibre filters used for sample collection were changed when the laser correction value dropped below 0.90 as recommended by the manufacturer. However, for specific periods we prolonged the use of the sample filter even if the laser correction factor was below 0.85 to test the influence of accumulation of mineral material on the sample filter to EC and OC determination. Regarding the efficiency of the denuder Arhami et al. (2006) determined the effect of the age of the filters in the denuder by side-by-side comparison of a denuder with fresh filters and one with 2-month-old strips. The results did not show a significant change after denuder strips were changed. Thus, filters in the denuder were changed after 3 months of use.

The Semi-Continuous OCEC analyzer deployed the EUSAAR2 thermal optical transmittance (TOT) protocol (Cavalli et al., 2010). OC and EC determined with the TOA method are defined as thermal OC and thermal EC and their sum representing Total Carbon, TC.

Real time BC concentrations were obtained by means of the AE33 Aethalometer (Magee Scientific) operating at 7 wavelengths (370, 470, 520, 590, 660, 880, 950 nm) equipped with a $PM_{2.5}$ inlet, and the MAAP 5012 (Thermo Fisher Scientific) equipped with a PM_{10} inlet. For the comparison with the Semi-Continuous OCEC analyzer the 880 nm wavelength Aethalometer data were converted to BC mass concentrations using the default mass attenuation cross section (MAC) of 7.77 $m^2\ g^{-1}$ given by the manufacturer. For MAAP BC the manufacturer suggested MAC of 6.6 $m^2\ g^{-1}$ was used to derive BC mass concentrations. Non-refractory PM_1 aerosol species (organic aerosols (OA), nitrate, sulfate, ammonium, chloride) were obtained with 30 min time resolution by an Aerosol Chemical Speciation Monitor (ACSM, Aerodyne Research Inc.) ACSM measurement periods with simultaneous and Semi-Continuous OCEC data were available compared from 22 Apr to 20 Jun 2016 at PR and from 29 Sep to 13 Dec 2016 at MSY. Additionally, $PM_{2.5}$quartz filter samples of 24 h duration were collected with both high volume (MCV) and low volume (DERENDA) samplers. A denunder was used in the $PM_{2.5}$ low volume sampler. A laboratory Sunset OCEC analyzer (TOT method and EUSAAR2 protocol) was used to analyze the 24 h $PM_{2.5}$quartz filters. Online analysis of TOT-OCEC in $PM_{2.5}$ (4 h time resolution), were compared with offline TOT-OCEC applying the EUSAAR2 temperature protocol. EC measurements (both thermal EC and optical EC) obtained with the Semi-Continuous OCEC analyzer were compared with BC from the MAAP 5012 and the AE33 Aethalometer. Weekly and daily trends of EC and OC measured with the Semi-Continuous analyzer and comparisons with the Aethalometer and MAAP BC data were conducted with the openair package (Carslaw and Ropkins, 2012). The format for all regressions is $y = ax + b$.

3. Results and discussion

3.1. OC and EC concentrations obtained by the Semi-Continuous analyzer

EC 4 h concentrations at PR were in the range 0.1–4.2 μgm^{-3} while OC ranged from 0.2 to 5 μgm^{-3}. At MSY, 4 h EC ranged from 0.01 to 1.8 μgm^{-3} and OC from 0.5 to 8.0 μgm^{-3} (Fig. 2). These values agree well with those previously reported in $PM_{2.5}$for other Spanish remote

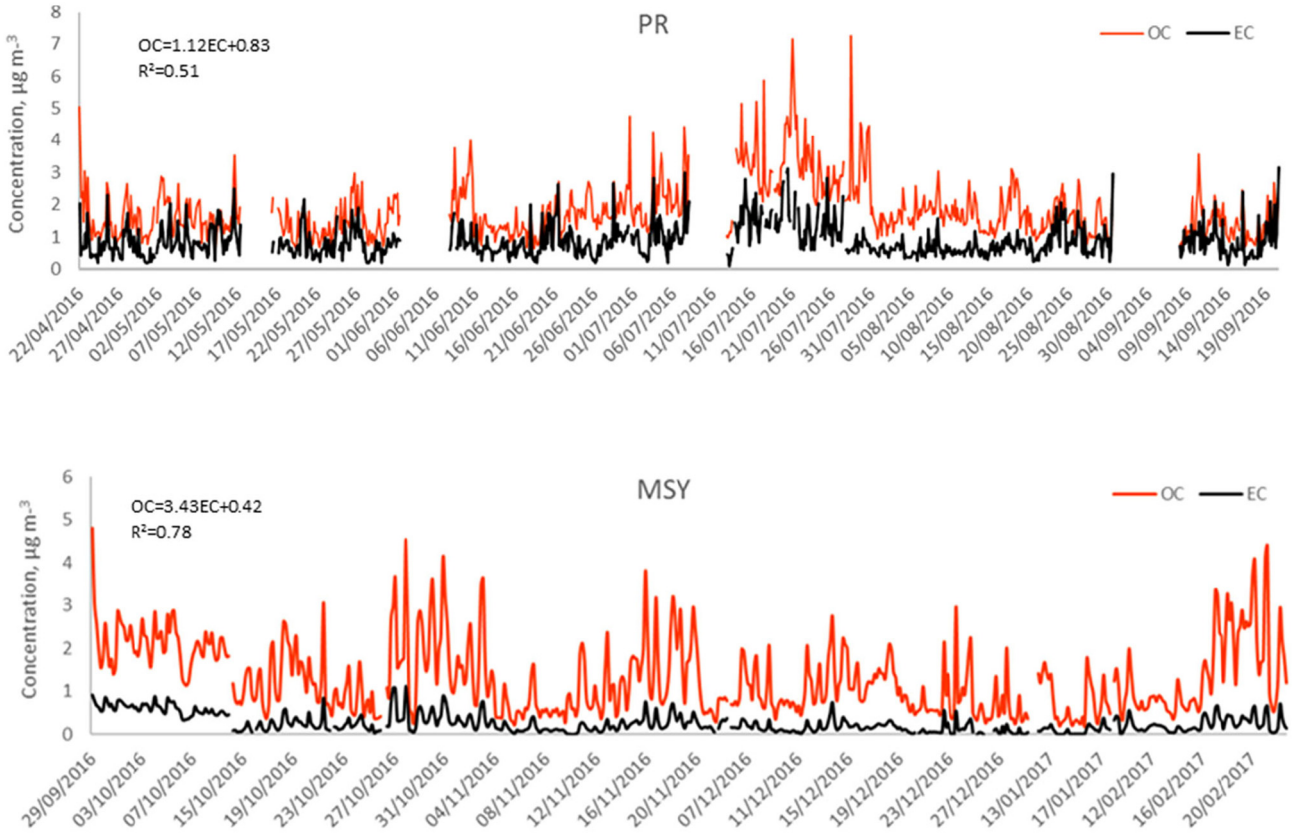

Fig. 2. Time series of OC and EC concentrations and OCvsEC regression equation in the urban background site of PR and in the regional site of MSY measured by the Semi-Continuous Sunset analyzer.

and urban background sites (Querol et al., 2013), European regional background sites (Cavalli et al., 2016) and European sites with similar characteristics (rural and urban background sites in Czeck Republick: Vodička et al., 2015; urban background site in northern France: Crenn et al., 2018).

The relationship between OC and EC can provide at some extent information regarding the common origin of carbonaceous aerosols (Turpin and Huntzicker, 1991). In this study, a good correlation was observed between OC and EC in $PM_{2.5}$in MSY site ($R^2 = 0.78$, a = 3.43, b = 0.42) while a moderate correlation, was found in PR site ($R^2 = 0.51$, a = 1.12, b = 0.83), Fig. 2 and Fig. S1. The higher correlations between EC and OC in the remote site suggest that both carbonaceous fractions were controlled by common sources and/or by different emissions but transported simultaneously to the receptor site. It confirms that the time series of EC and OC concentrations in MSY site were modulated by meteorology, air masses circulation and transport of urban and regional pollutants (Pandolfi et al., 2014). The weak correlation in the urban background site indicates that, in addition to primary traffic sources of OC and EC, other emission sources may have contributed significantly. Reche et al. (2011) demonstrated that traffic is the most important source of BC (and EC) in the urban site studied here, and from that study BC levels have been reduced by around 50%. This behaviour has been previously observed in several sites across Europe. At traffic and urban background sites OC and EC correlations were not as marked as for the rural sites, probably due to the presence and different impact of multiple sources (Querol et al., 2013). Nevertheless, it should be noted that sampling in the two sites was not simultaneous but took place in different periods: during the warm period in PR and during cold season in MSY. This has probably influenced the correlation between OC and EC as in general, correlation is stronger during the cold months than in the warm season (Cesari et al., 2018). Regarding the OC/EC ratio this can range from low values (about 1) in polluted areas to high values up to 15 in remote locations (Querol et al., 2013; Sandrini et al., 2014). The OC/EC ratios, for MSY and PR sites, ranged between 1.8 and 12.8 and 0.7 to 8.1 respectively, (Fig. S2). The higher ratios for MSY are attributable to a relative high proportion of primary and secondary biogenic aerosols, and the secondary organic aerosol (SOA) also from an anthropogenic origin (Minguillón et al., 2015), as opposed to the relatively lower relative SOA contribution at PR, even during summer months (Minguillón et al., 2016).The weekly and daily patterns for OC and EC in $PM_{2.5}$ for MSY and PR sites are shown in Fig. S3. At PR, EC reached higher concentrations during weekdays with a clear decrease on weekends due to lower local emissions from road traffic. The weekly pattern of OC was slightly different. Higher OC concentrations were observed from Thursday to Saturday and lower from Sunday to Tuesday suggesting that the changes in road traffic emissions that control EC concentrations did not significantly impact on OC concentrations otherwise similar changes in the weekday distribution of OC would be observed. At MSY both EC and OC weekly pattern were relatively uniform, without observing an evident weekly trend. The daily evolution of EC in PR followed the same trend as road traffic emissions with a bimodal distribution peaking in the morning hours from 6 to 9 h and in the early noon from 18 to 21 h (local time), and decreasing notably during the middle hours of the day (Querol et al., 2013; Reche et al., 2011). This pattern was not marked on weekends where only the early noon peak was observed again following the daily trend of vehicle emissions with higher traffic flow after 18 h. OC concentrations showed variable daily distributions. There was an early morning OC peak during week-days that coincides with the EC peak. Afterwards, OC concentrations declined to increase again during the afternoon and remained rather stable until night. This trend reflected the impact that primary emissions had on OC levels since the first OC peak appeared with the peak in traffic flow, and also the formation of SOA influenced by meteorological conditions and gaseous precursors. Weekends had a single-mode distribution with OC concentrations peaking during midday hours from 10 to 14 h. At MSY, OC and EC reached the maximum daily values in the early noon due to the transport of urban emissions and formation processes of organic aerosol (Minguillón et al., 2015; Pandolfi et al., 2014; Querol et al., 2013).

3.2. Sunset Semi-Continuous analyzer vs sunset laboratory analyzer

To assess the precision, stability and comparability of the measurements we calculated the limit of detection (LOD) for OC and EC of the Semi-Continuous OCEC analyzer and the laboratory OCEC analyzer. LOD was determined by calculating the average instrument blank filter value (calculated from 40 blank measurements) plus two times its standard deviation (SD) as recommended in EN16909:2017. LOD for OC was 0.04 μgm^{-3} and 0.03 μgm^{-3} for the Semi-Continuous and offline analysers respectively while LOD of EC was 0.01 μgm^{-3} for both analyzers. The OC and EC values lower than the corresponding LOD threshold were excluded from the statistical calculations. Measurement uncertainties were calculated using the method described in EN16909. The combined relative standard uncertainty of OC average values was 12% while for EC average concentrations was 18% for both analyzers. Fig. 3 compares the 24-h averaged OC and EC measurements of the Semi-Continuous Sunset analyzer with the OC and EC concentrations determined in $PM_{2.5}$ 24 h filters (offline concentrations) from the low volume sampler equipped with a denuder and the high volume sampler (without denuder) for the two sampling sites. The offline measurements were blank corrected using laboratory blanks for OC and EC analysis but the Semi-Continuous measurements have not been blank corrected. In PR site, both samplers had slopes close or equal to unity (Fig. 3, Panel A). The regression for EC reached $R^2 = 0.83$, a = 0.93 and b = 0.07 for the low volume sampler. For the high volume sampler, the regression reached $R^2 = 0.84$, a = 1.04 and b = 0.05. Previous studies have considered the intercept of the regression as the instrument blank (Bae et al., 2004). The intercepts of 0.07 and 0.05 were higher than the instrument blanks of the Semi-Continuous analyzer obtained by collecting samples with zero sample volume that were constantly found in the range of 0.00–0.01 $\mu g\ cm^{-2}$ of carbon. These results confirm that the Semi-Continuous measurements of EC correlate very well with the laboratory based measurements and no blank correction is needed. The difference observed between the two slopes, though small cannot be explained by the use of denuder or not since EC is not affected by positive or negative artefacts. Correlations for OC regressions were strong, $R^2 = 0.81$ and 0.84 for the low volume and high volume, respectively, with a = 0.99 and b = −0.18 for the low volume and a = 0.93 and b = 0.12 for the high volume samples. It was expected to find better agreement with the low volume sampler since the Semi-Continuous analyzer also contains a denuder to remove the VOCs potentially causing positive OC adsorption artefacts. The high volume sampler is expected to present low positive artefacts because of high face velocity but negative artefacts should neither be neglected (Karanasiou et al., 2015; Viana et al., 2006). The b = 0.12 with the high volume sampler could be attributed to OC losses through volatilization of semi-volatile organic compounds (SVOCs). On the other hand, the b = −0.18 obtained for the low volume samples cannot be explained. Other sources of uncertainty such as fluctuations of the flow rate resulting in changes in the collection efficiency of the different $PM_{2.5}$samplers could explain the observed intercepts.

Similarly, in the regional background site the correlation for EC was very good; $R^2 = 0.89$ for the denuded low volume sample and 0.77 for the undenuded high volume sample. The slope of the regression with the denuded and undenuded samples was a = 0.91 and 1.02 correspondingly (Fig. 3, Panel B). The obtained intercepts were negligible reflecting the low blank values of EC. The regression of OC reached $R^2 = 0.78$ for both samplers and slopes close to 1 (a = 1.03 for the high volume and 0.95 for the low volume sampler). As observed in PR, the difference between the two slopes cannot be explained. Surprisingly, online OC had marginally better agreement with the undenuded offline OC

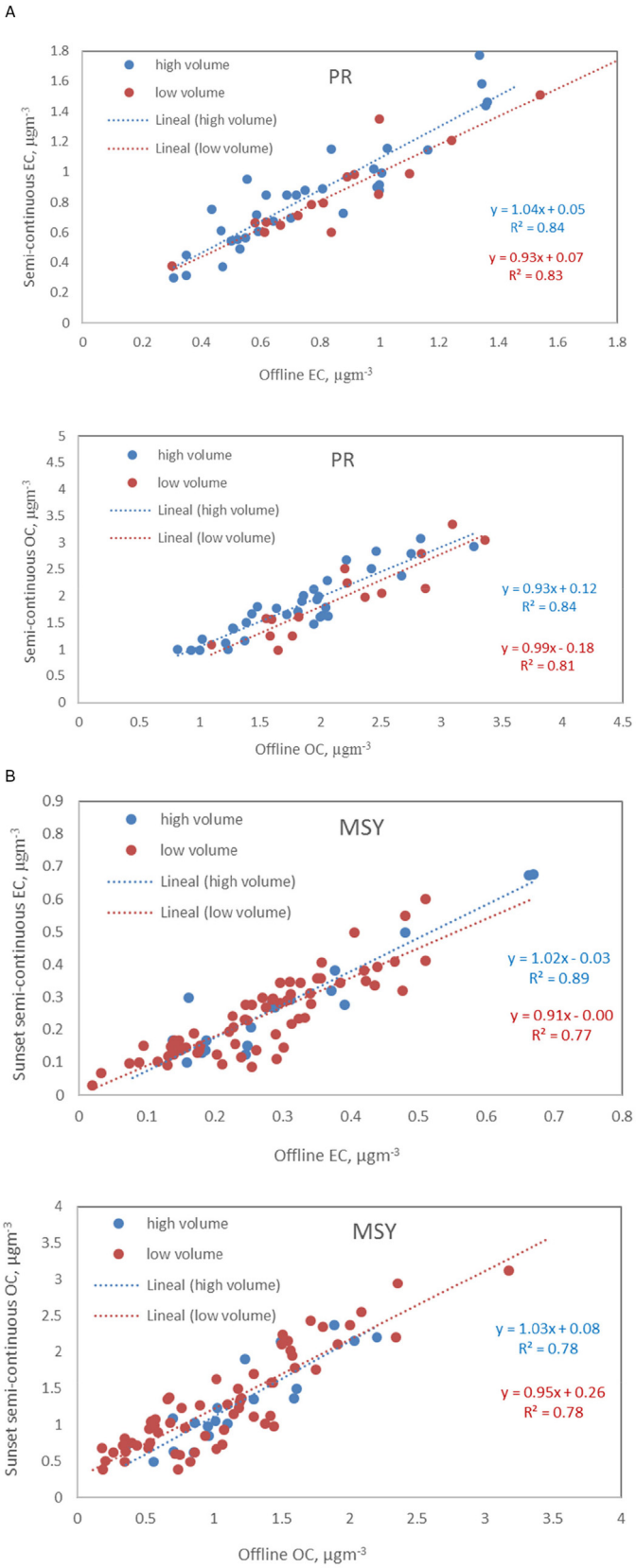

Fig. 3. Comparison of 24 h average Semi-Continuous EC and OC measurements and the offline ECOC measurements at 24 h filters collected with a denuded low volume sampler (red regression line) and undenuded high volume sampler (blue regression line) at the Palau Reial (PR) urban background site, (Panel A) and at the Montseny (MSY) regional background site, (Panel B).

concentrations as indicated by the lower intercept (b = 0.08) compared to that of the denuded samples (b = 0.26).

These results indicate that operating the ECOC Semi-Continuous analyzer with the EUSAAR2 protocol yields very good agreement with 24-h offline OC and EC measurements from the laboratory OCEC analyzer for both denuded and undenuded filter samples at both sites.

3.3. Sunset Semi-Continuous thermal EC, Aethalometer BC, and MAAP BC

The comparison of EC from the Semi-Continuous OCEC analyzer and BC from absorption measurements can provide an insight on their relationship and variability in the two monitoring sites. BC measurements obtained by the Aethalometer (at 880 nm) were in very good agreement with thermal EC concentrations of the Semi-Continuous OCEC analyzer at both sampling sites, Fig. 4. The ordinary least square linear regression was used as a method of comparison. Thus, R^2 reached 0.79 and 0.94 for PR and MSY respectively. The slope (a) of the regression between BC and EC was 1.2 for PR and 1.9 for MSY site (b = 0.19 and −0.04, Fig. 4, Panel A). The observed slopes indicate that the Aethalometer BC levels were higher (when using the MAC provided by the manufacturer) than thermal EC concentrations, which is in agreement with earlier studies that compared collocated measurements of the Aethalometer (using the manufacturer MAC value) and the Semi-Continuous OCEC analyzer. Healy et al. (2017) found BC mass concentrations constantly higher than EC concentrations by a factor of 1.7. In New York, Rattigan et al. (2010) found a consistent seasonal difference in BC vs EC slopes over three years, with slopes of 1.4 and 2.0 in the cold and warm period respectively. In Shangai, BC vs EC slopes ranged from 1.3 to 1.7 (Chang et al., 2017). In these previous studies NIOSH-like protocols were deployed by the Semi-Continuous OCEC analyzer except in one study (Healy et al., 2017) where a hybrid protocol of the NIOSH-like and EUSAAR2 protocol was used. There is no previous study reporting on the correlation between Sunset online EC with EUSAAR2 and Aethalometer BC. Differences between the two type of measurements are expected since the BC and EC concentrations are based on two different measurement techniques (Massling et al., 2015). As mentioned previously, the optical attenuation values measured by the Aethalometer were converted to BC mass concentration by using the

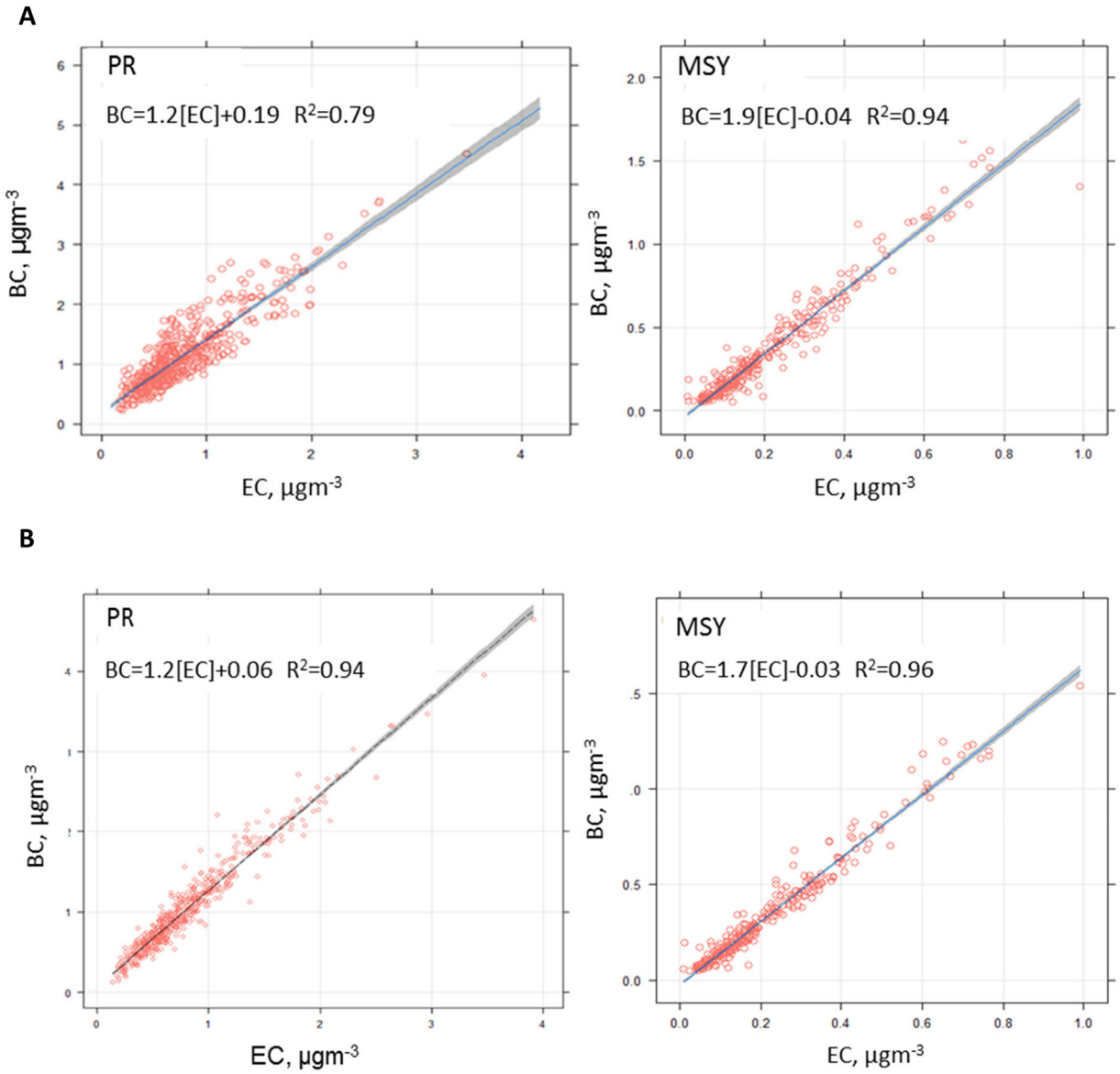

Fig. 4. 4 h-averaged Aethalometer BC (measured at 880 nm) compared to Semi-Continuous Sunset thermal EC concentrations at Palau Reial Urban background site (PR) and Montseny regional background site (MSY) (Panel A) and 4 h-averaged MAAP BC compared to Semi-Continuous Sunset thermal EC concentrations at Palau Reial Urban background site (PR) and Montseny regional background site (MSY) (Panel B).

instrument MAC of 7.7 m^2g^{-1} at 880 nm. However, several studies have suggested that optical analysis for BC requires calibration for site-specific aerosols since the absorption coefficient depends on the size distribution, type of aerosol mixtures, deposited mass per unit time and chemical characteristics of light absorbing species that could include OC as well as EC (Jeong et al., 2004). The MAC varies from 6.5 to 13 m^2g^{-1} across regional sites in Europe (Zanatta et al., 2016). Using a manufacturer provided coefficient MAC yields deviated BC concentrations. BC is in fact measured as equivalent BC (EBC, but used BC for simplicity) which means that BC should be equal to EC (Petzold et al., 2013) and to this end experimental MACs should be obtained in situ for each site. The deviation obtained means that the manufacturer provided MAC should be replaced by the one obtained at each site.. Furthermore, the higher slope in MSY site can be attributed to the fact that BC transported toward MSY is efficiently internally mixed with non-absorbing or less-absorbing particles (such as sulphates, organic matter) compared to the urban background site. These coatings increase the MAC of BC measured in remote areas compared to the MAC of freshly emitted BC measured in urban sites with respect to EC mass (Zanatta et al., 2016). Thus, the lensing effect is enhanced at the remote site leading to higher BC than EC concentrations.

Fig. 4 (panel B) shows the comparison between BC measured with the MAAP and thermal EC for the two sites. As observed for the Aethalometer MAAP BC concentrations were also higher than the thermal EC although strongly correlated ($R^2 = 0.94$, a = 1.2, b = 0.06 at PR and $R^2 = 0.96$, a = 1.7, b = −0.03 at MSY). Thus the obtained slopes of 1.2 and 1.7 for PR and MSY, respectively were comparable with those found in previous evaluations between the Sunset thermal EC using NIOSH-like or IMPROVE protocol and the MAAP BC (again using the MAC from the manufacturer) ranging from 1.4 to 2.2 (Cesari et al., 2018; Park et al., 2006; Kanaya et al., 2008). Thus, again the observed differences between the thermal EC and the MAAP BC can be linked to the use of the default MAC and not a site-specific one, to the use of a PM_{10} inlet in the MAAP instead of $PM_{2.5}$ like in the Sunset OCEC analyzer, and for the MSY site to the BC absorption enhancement (higher MAC) due to aging of BC particles and consequent internal mixing of BC with non-absorbing particles.

3.4. Semi-continuous sunset optical EC and BC

Except from the thermally determined EC and OC, the Semi-Continuous analyzer is also providing the so-called optical EC using the transmittance measurements of the laser beam (658 nm) through the filter during sampling. A predetermined calibration coefficient is used to convert laser attenuation to EC mass on the filter. This value is reported every minute as optical EC. Overall, the optical EC obtained from the Sunset Semi-Continuous analyzer correlated very well with the BC from the Aethalometer as clearly seen in the scatter plots in Fig. 5. In PR we used 5-min averages while in MSY the data were 4 h-averaged because of many EC values below EC LOD (<0.01 μgm^{-3}). The R^2 reached 0.80 in PR and 0.94 in MSY. Similarly to thermal EC, the Sunset optical EC was consistently lower than the Aethalometer BC at both sites. The obtained slopes of 1.3 in PR and 1.4 in MSY (and b = 0.16 and 0.01, respectively) are in agreement with previous studies. In Prague, Zíková et al. (2016) found that Sunset optical EC and BC from a collocated MAAP were fairly comparable (within 9%) and had a high correlation ($R^2 > 0.92$) during one-year measurements. Brown et al. (2019) compared Sunset optical EC with an Aethalometer in CSN in the United States. Good correlations ($R^2 > 0.70$) were obtained for concentrations up to 2 $\mu g\ m^{-3}$. The slopes varied between the sampling sites ranging from 1.4 to 2.3 (b = 0.05 to 0.14). At an urban site in New York, optical EC was strongly correlated with Aethalometer BC ($R^2 = 0.93$), with slope of 1.7 (Venkatachari et al., 2006). The Sunset optical EC is determined by the light absorbance using a 658 nm laser, while the Aethalometer measures light absorption at 880 nm. This difference might account in part for the higher BC values as compared to the optical EC values. Whereas for PR thermal EC was very similar to optical EC as the BCvsEC slopes were 1.2 and 1.3, for thermal EC and optical EC, respectively; at MSY the corresponding slopes were 1.7 and 1.4, pointing out that the difference between thermal and optical EC was larger at MSY.

3.5. Semi-continuous sunset OC and ACSM OA

OC measurements obtained with the Semi-Continuous Sunset analyzer (with NIOSH-like protocol) have typically been comparable to other measurements of carbonaceous aerosol, such as from the Aerosol Mass Spectrometer (AMS). Brown et al. (2013) found that AMS OC and Sunset OC were very well correlated with slope of 0.91. In Hong Kong, Lee et al. (2013) also found good agreement between Sunset and AMS measurements ($R^2 = 0.87$, a = 0.88). In Northern France, Crenn et al. (2018) found correlations between HR-ToF-AMS OC and Sunset OC with $R^2 = 0.50$ to 0.92, a = 0.29 to 0.61, depending on season and type of site. Other studies found weaker correlations

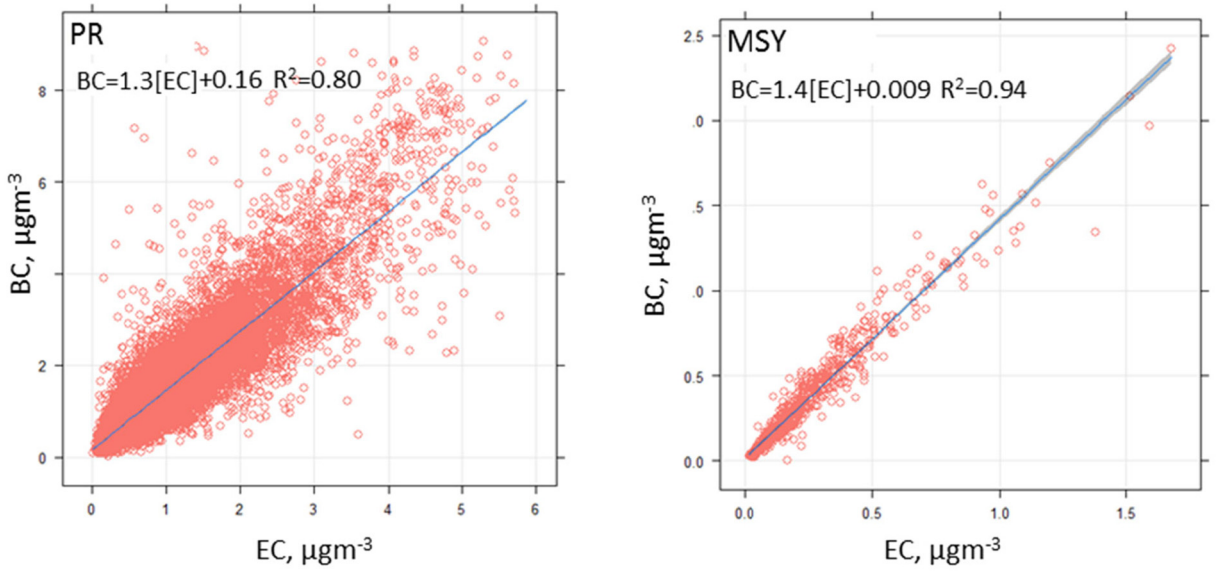

Fig. 5. Averaged Aethalometer BC (measured at 880 nm) compared to Sunset optical EC concentrations at Palau Reial Urban background site (PR) and Montseny regional background site (MSY).

and higher variability between AMS and Sunset measurements, R^2 = 0.53–0.67, a = 0.71 to 1.79 (Docherty et al., 2011; Takegawa et al., 2005). Budisulistiorini et al. (2014) found strong correlations between ACSM OA with OC from the Sunset analyzer (R^2 = 0.86 and 0.92, a = 4.85 and 3.85, for summer and fall, respectively), with slopes being interpreted as OM/OC ratios. The high OM/OC ratios were attributed to underestimation of OC by offline techniques and/or to overestimation of OA by the ACSM due to the use of default Relative Ionization Efficiency (RIE), which may differ from the real ones, as shown later by Xu et al. (2018).

In the present study, $PM_{2.5}$OC online measurements were correlated with the PM_1 OA concentrations calculated from the ACSM data. The slope of the linear fit may be interpreted as the OA/OC ratio (Fig. 6). Nevertheless, due to the different size fractions between measurements, the absolute value of the ratio should be interpreted with caution. Previous comparisons between OA from ACSM with PM_1 OC from offline filter samples at MSY have resulted in higher ratios (4.25, Minguillón et al., 2015), leading to the conclusion of overestimation of OA by ACSM due to underestimation of RIE, in agreement with Budisulistiorini et al. (2014). The higher ratio at MSY (a = 2.3, b = −0.37, R^2 = 0.84) than at PR (a = 1.9, b = −0.44, R^2 = 0.80) is consistent with the higher degree of oxidation due to prevalence of SOA is consistent with the higher degree of oxidation due to prevalence of SOA at the regional site.

3.6. Split point and accumulation of metals

Biases in the determination of OC and EC by thermal-optical analysis have been previously reported in Karanasiou et al. (2015). Uncertainties concerning the split between EC and OC are influenced by the aerosol type and chemical composition. The presence of certain minerals can complicate the optical correction for pyrolysis. Chow et al. (2001) and Fung et al. (2002) demonstrated that mineral components, such as Fe-oxide might provide oxygen and cause oxidation of some EC at high inert-mode temperatures. Giannoni et al. (2016) found that the split point falls in the inert mode for samples from regional background sites analyzed with a NIOSH-like protocol reaching 870 °C in the He phase. This phenomenon would be negligible for EUSAAR2 protocol given that the EUSAAR2 maximum temperature in the inert mode (650 °C) is lower than the corresponding one in a NIOSH-like protocol. Nevertheless, Panteliadis et al. (2015) observed pre-oxidation of EC in the inert mode for a NIOSH-like protocol and also for the EUSAAR2 protocol.

Thus, it is possible that some refractory mineral oxides will accumulate on the filter of the Semi-Continuous Sunset OCEC analyzer and might alter laser transmittance. To determine the split point, the Sunset software multiplies the initial laser signal by a laser correction factor to account for changes in laser transmittance as a function of temperature. The laser correction factor is calculated from the variation in the laser transmittance during the cooling of the oven when analysis is finished. Hence, the laser correction factor can be used as an indicator of the aging of the quartz filter of the OCEC analyzer as it usually decreases with the accumulation of refractory material on the filter. Very few studies have investigated the presence of refractory material regarding the effect of the refractory particles on the formation of PC and split point variation. Arhami et al. (2006) found negligible effect on the measured OC and EC concentrations when using a week-old filter versus a fresh filter. A study conducted in Beijing (Jung et al., 2011) suggested that the accumulated refractory material on the filter may play an important role in the EC measurement, by altering the split point, the formation of PC, and consequently evolution of EC and PC. In the present study, the filter of the OCEC analyzer was changed when the laser correction factor dropped below 0.90. However, desert dust events were quite frequent during the campaigns leading to fast decrease of the laser correction factor. We examined the effect of metals accumulation on the split point and on PC formation by plotting split time and PC as a function of the laser correction factor, for the two sampling sites, Fig. 7. In the urban background site, the split times and PC slightly decreased as the laser correction factor decreased from 0.95 to 0.90, suggesting the enhanced formation of PC on the new quartz filter, and then varied independently from the laser correction factor values. For filters highly loaded with refractory material (laser correction factor < 0.80), the split point was found in the inert mode (<660 s) and PC formation was negligible. This is usually observed in samples where pre-oxidation occurs resulting in early desorption of PC and/or EC. Fe-oxides in the urban area are highly increased versus the regional background due to contributions from the wear of the vehicles brake disk and pads, and in both cases by desert dust contributions, having higher Fe contents than local dust (Amato et al., 2016; Querol et al., 2001). In the present study Fe $PM_{2.5}$ average concentrations were 150 ng/m^3 in the urban background site while in the remote site were 30 ng/m^3. Furthermore, during the periods that the laser correction factor was rapidly decreased Fe levels reached their maximum values found in the range 140–240 ng/m^3. Thus, a catalytic effect was caused from Fe and premature oxidation shifted the split point in the inert mode.

A different pattern was observed in MSY, Fig. 7. Higher PC values were observed while the split time always fell in the oxidized mode

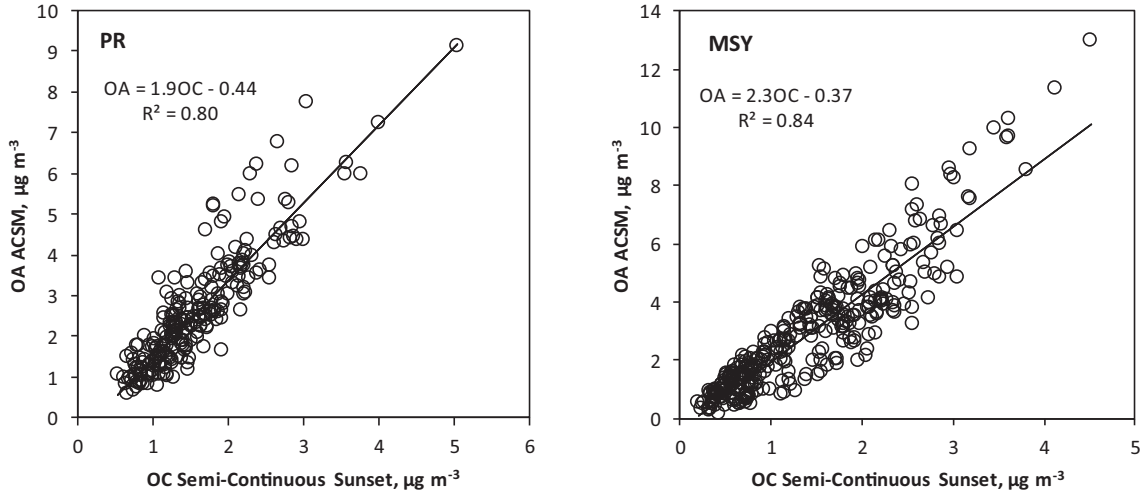

Fig. 6. Correlation of PM_1 OA concentrations as obtained by the ACSM and $PM_{2.5}$ OC (µgm^{-3}) of the Sunset Semi-Continuous OCEC analyzer at the Palau Reial urban background (PR) and Montseny regional (MSY) sites.

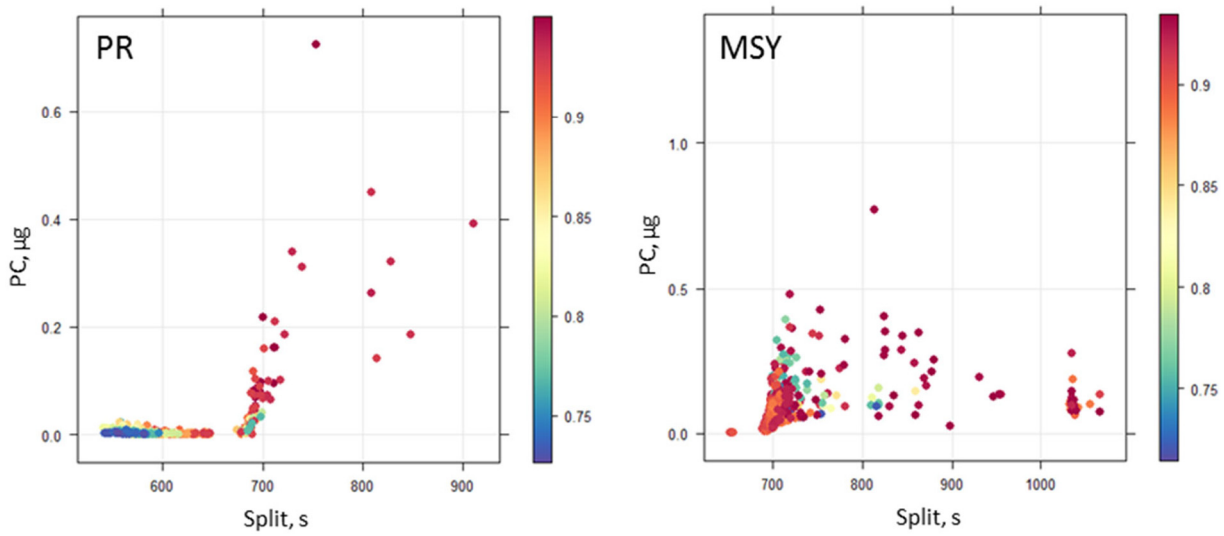

Fig. 7. OC-EC split times and PC as a function of the laser correction factor (color scale) at Palau Reial Urban background site (PR) and Montseny regional background site (MSY).

(after 660 s). Generally, more PC is formed in regional background site where biomass burning activities enhance BrC levels that consequently can increase PC generated during the analysis (Reisinger et al., 2008). There was no clear evidence that the decrease in the laser correction factor influenced the formation of PC and or the split between OC and EC.

Fig. 8 (Panel A) shows the thermograms of two selected samples from PR site. The first sample was measured on May 17, 2016 (at 20:00 LT) with a fresh filter and laser correction of 0.94 and the second one was measured on May 25, 2016 (at 08:00 LT) with an aged filter and laser correction factor of 0.85. The initial laser transmittance for the aged filter was much lower than the corresponding value in the fresh filter attributable to the coloring of the filter from the accumulation of crustal material. The two samples had similar OC but different EC and PC values. PC formation was observed for both samples since the transmittance decreased noticeably in the inert mode. In the fresh filter the split between OC and EC was at 736 s in the oxidized mode correctly attributing the PC peak to OC. However, the split point for the aged filter fell in the inert mode (610 s) before the introduction of the oxidized atmosphere. Thus, the PC peak was erroneously accounted as EC. This could result from the presence of mineral oxides on the filter leading to the oxidation of PC and/or EC in the He mode.

At MSY we did not observe any shift of the split point and/or changes on PC formation due to the presence of refractory material on the filter. The thermograms of two selected samples are given on Fig. 8 (Panel B). The first sample was measured on October 15, 2016 (at 20:00) with a fresh filter and laser correction of 0.94 and the second one was measured on October 25, 2016 (at 08:00) with an aged filter and laser correction factor of 0.78. Even though the two filters had very different laser correction factors, the initial laser transmittance was not that different (14,000 for the fresh filter and 12,000 for the aged filter). In both samples, the split point fell in the oxidized mode with no indication of premature evolution of EC from mineral oxides.

3.7. Desert dust events

Desert dust can influence TOA due to the presence of carbonate carbon (CC) that depending on its characteristics could evolve in the inert mode as OC or in the oxidized mode as EC; and to the high contents of Fe-oxides, that can prematurely oxidize EC. If not accounted for, the interference of CC with the OC or EC signal can lead to an overestimation of the OC or EC concentration. Karanasiou et al. (2011) demonstrated that with the EUSAAR2 thermal protocol, more than 95% of CC evolves as OC during the maximum temperature step in inert mode for CC amounts up to 56 µg, corresponding to the mass of CC that could be collected during extreme desert dust events (PM_{10} concentration above>200 μgm^{-3}). During the experimental campaign at MSY an extreme dust outbreak occurred over the whole Iberian Peninsula from 20th to 25th February 2017. Even though winter is the season when dust intrusions are less frequently observed across the Mediterranean basin (Pey et al., 2013; Querol et al., 2019), some extreme dust outbreaks, as the one described here or others more recent (e.g. 23rd January 2020, Barcelona) have occurred during the cold season. On 22nd February 2017 PM_{10} concentrations in MSY reached 280 μgm^{-3} (Titos et al., 2017). Fig. 9 shows the thermogram of a sample measured on 22nd February 2017 at 16:00 h (LT) from MSY during the dust outbreak. An uncommon peak distribution in the He mode was observed. The peak in the last temperature step of the He mode (OC4) was higher and wider than usual (see Fig. 8) thus, could be attributed to CC. The upper limit CC amount calculated from Ca concentrations on 22nd February (if both Ca and CC are entirely present as $CaCO_3$) was 0.6 μgm^{-3} while OC4 concentration was higher, equal to 1.1 μgm^{-3}. It is possible that most of the CC evolved during the maximum temperature of the He mode simultaneously with organic compounds leading to an overestimation of total OC. This demonstrates that it is advisable to examine carefully TOA thermograms when dust events occur to consider interferences from CC.

4. Conclusions

This work studied the performance of the EUSAAR2 protocol with the Semi-Continuous OCEC analyzer at two challenging environments, an urban background site influenced by traffic emissions and a regional background site. The comparison of the 24-h averaged OC and EC measurements of the Semi-Continuous analyzer with the OC and EC concentrations determined offline in $PM_{2.5}$24h filters yielded very good agreement for both denuded (low volume sampler) and undenuded samples (high volume sampler). In the urban background site, the regression for EC reached $R^2 = 0.84$ and 0.83, a = 0.93 and 1.04, and b = 0.05 and 0.07, for the low volume and high volume samplers respectively. In the remote site the slope of the EC regression with the undenuded and denuded samples reached $R^2 = 0.89$ and 0.77, a = 1.02 and 0.91, and b = −0 and − 0.03, correspondingly. For OC, the slopes were a = 0.99 for the low volume ($R^2 = 0.81$, b = −0.18) and a = 0.93 ($R^2 = 0.84$, b = 0.12) for the high volume samples at the urban site and a = 0.95 ($R^2 = 0.78$, b = 0.26) and a = 1.03 ($R^2 = 0.78$, b = 0.08) for the low and high volume samples respectively at the regional background.

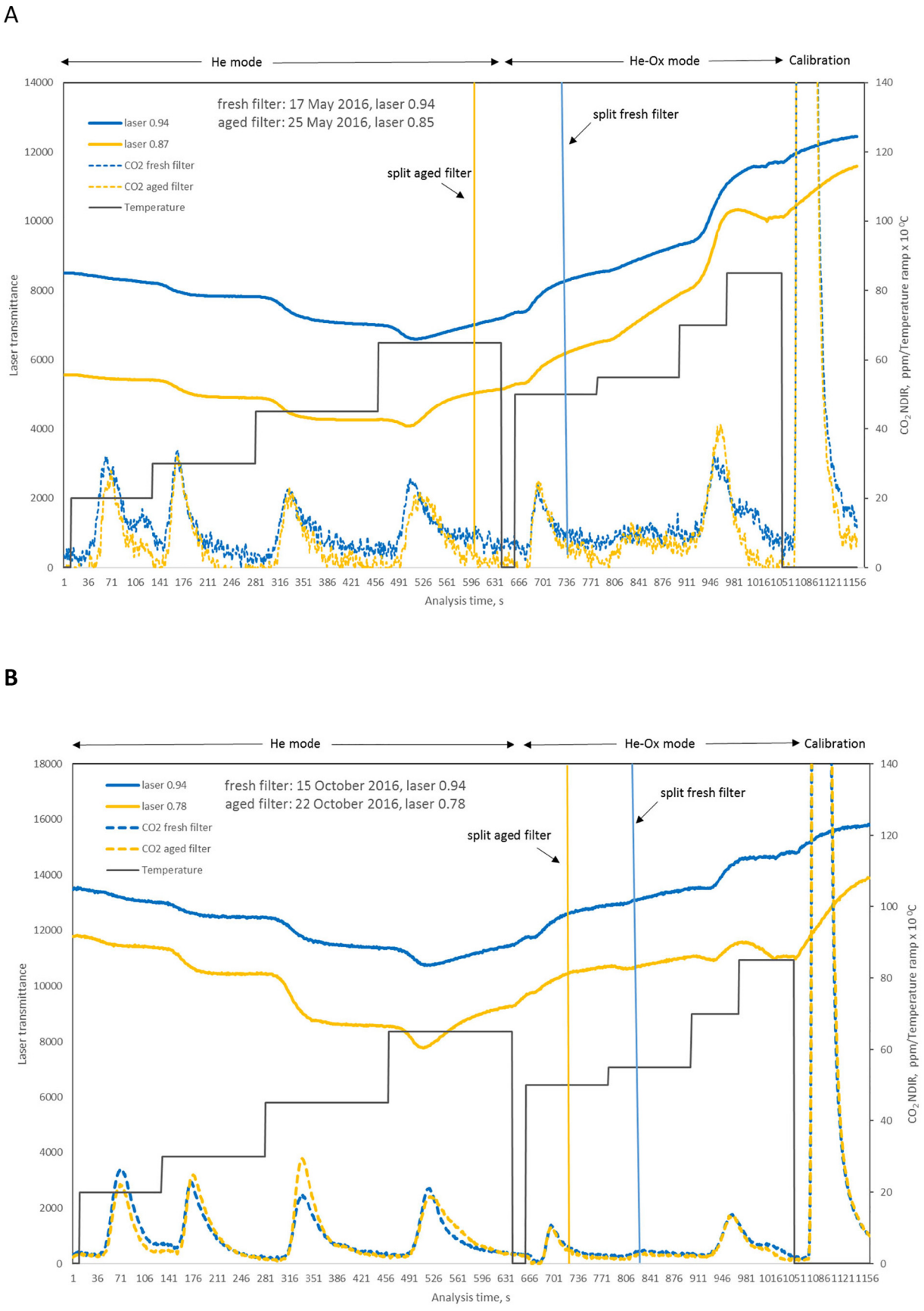

Fig. 8. Thermograms for fresh filter measured on May 18, 2016 at 20:00 with laser correction factor equal to 0.94 (blue color) and aged filter measured on May 25, 2016 at 8:00 with laser correction factor equal to 0.85 (orange color) from Palau Reial urban background site (PR), (Panel A) and thermograms for fresh filter measured on October 15, 2016 at 16:00 with laser correction factor equal to 0.94 (blue color) and aged filter measured on October 27, 2016 at 20:00 with laser correction factor equal to 0.78 (orange color) from Montseny regional background site (MSY), (Panel B).

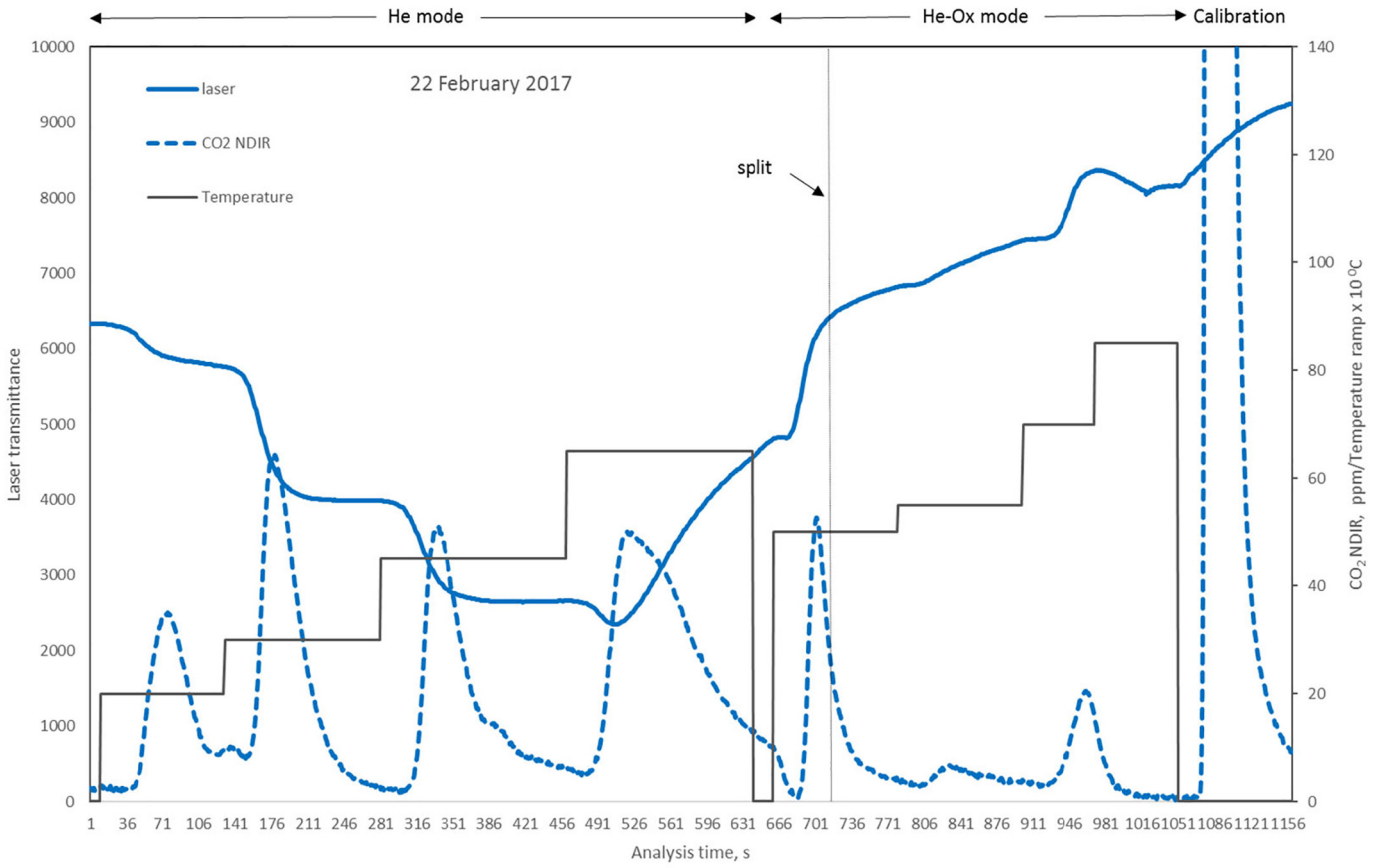

Fig. 9. Thermogram of a sample measured on 22nd February 2017 at 16:00 h LT from Montseny regional background (MSY) during the dust outbreak.

BC measurements obtained by the Aethalometer and MAAP were in very good agreement with EC at both sampling sites. BC levels were consistently higher than EC as indicated by the slope of the regression (slope and intercepts of Aethalometer BC vs EC a = 1.2 and b = 0.19 for the urban site and a = 1.9 and b = 0.04 for the regional background site; MAAP BC vs EC a = 1.2 and b = 0.06 for the urban site and a = 1.7 and b = 0.03 for the regional site). The slopes different from unity, as also observed in prior studies, confirm the need of using the site-specific mass absorption coefficients (MACs) to convert absorption measurements to BC mass concentrations. Similarly, the optical EC obtained from the Semi-Continuous analyzer correlated very well with Aethalometer BC data. The fact that thermal EC (with the EUSAAR2 protocol) and optical EC is quite comparable to BC indicates that both are reliable measurements and can be considered in monitoring networks. The comparison of OC concentrations by the Semi-Continuous Sunset analyzer with organic aerosol online measurements by ACSM showed strong correlations and OA/OC values of 1.87 and 2.3 for the urban and regional background sites, respectively.

We detected shift of the split point to the inert mode and changes on PC formation and evolution due to the accumulation of refractory material as a result of prolonged periods of sampling on the same filter only in the urban background site. This could result from the presence of mineral oxides on the filter leading to the oxidation of PC and/or EC at lower temperatures in the He mode. During an extreme dust outbreak, we observed the evolution of CC in the He mode leading to the overestimation of OC. In case of desert dust intrusions, the thermograms should be examined carefully to detect any unusual patterns to account for interferences from CC. If calcium concentration data are available an estimation of the maximum CC value evolving in the He mode would permit assessment of OC overestimation.

Generally, the Sunset Semi-Continuous analyzer with EUSAAR2 provided robust and consistent measurements with offline TOT method. When interferences from refractory material are considered the Sunset analyzer is suitable for routine monitoring networks.

CRediT authorship contribution statement

A. Karanasiou: Conceptualization, Investigation, Validation, Formal analysis, Writing - original draft, Writing - review & editing. **P. Panteliadis:** Methodology, Investigation, Validation. **N. Perez:** Investigation, Validation, Data curation. **M.C. Minguillón:** Investigation, Validation, Writing - review & editing. **M. Pandolfi:** Investigation, Validation, Writing - review & editing. **G. Titos:** Formal analysis, Writing - review & editing. **M. Viana:** Writing - review & editing. **T. Moreno:** Writing - review & editing. **X. Querol:** Resources, Writing - review & editing. **A. Alastuey:** Conceptualization, Resources, Supervision.

Declaration of competing interest

The authors declare that they have no known competing financial interests or personal relationships that could have appeared to influence the work reported in this paper.

Acknowledgements

This work was partially supported by ACTRIS-2 Trans-National Access TNA grant “Evaluation of Semi-Continuous OCEC analyzer performance with the EUSAAR2 protocol”, SCOPE; the “Agencia Estatal de Investigación” from the Spanish Ministry of Science, Innovation and Universities under the project CAIAC (PID2019-108990RB-I00), and by the Generalitat de Catalunya (AGAUR 2017 SGR41). A. Karanasiou, M. Pandolfi and M.C. Minguillón are funded by Ramón y Cajal Fellowships (RYC-2014-16885, RYC-2013-14036,

RYC-2015-18458) awarded by the Spanish Ministry of Economy and Competitiveness cofunded by the European Social Fund. This work was supported by the Spanish Ministry of Science and Innovation (Excelencia Severo Ochoa, Project CEX2018-000794-S).

Appendix A. Supplementary data

Supplementary data to this article can be found online at https://doi.org/10.1016/j.scitotenv.2020.141266.

References

Amato, F., Alastuey, A., Karanasiou, A., Lucarelli, F., Nava, S., Calzolai, G., Severi, M., Becagli, S., Gianelle, V.L., Colombi, C., Alves, C., Custódio, D., Nunes, T., Cerqueira, M., Pio, C., Eleftheriadis, K., Diapouli, E., Reche, C., Minguillón, M.C., Manousakas, M.-I., Maggos, T., Vratolis, S., Harrison, R.M., Querol, X., 2016. AIRUSE-LIFE+: a harmonized PM speciation and source apportionment in five southern European cities. Atmos. Chem. Phys. 16, 3289–3309. https://doi.org/10.5194/acp-16-3289-2016.

Arhami, M., Kuhn, T., Fine, P.M., Delfino, R.J., Sioutas, C., 2006. Effects of sampling artifacts and operating parameters on the performance of a semicontinuous particulate elemental carbon/organic carbon monitor. Environ. Sci. Technol. 40, 945–954.

Bae, M.S., Schauer, J.J., DeMinter, J.T., Turner, J.R., Smith, D., Cary, R.A., 2004. Validation of a semi-continuous instrument for elemental carbon and organic carbon using a thermal-optical method. Atmos. Environ. 38, 2885–2893.

Bauer, J.J., Yu, X.Y., Cary, R., Laulainen, N., Berkowitz, C., 2009. Characterization of the sunset Semi-Continuous carbon aerosol analyzer. J Air Waste Manag Assoc 59 (7), 826–833 Jul.

Birch, M.E., 1998. Analysis of carbonaceous aerosols: interlaboratory comparison. Analyst 123, 851–857.

Birch, M.E., Cary, R.A., 1996. Elemental carbon-based method for monitoring occupational exposures to particulate diesel exhaust. Aerosol Sci. Technol. 25, 221–241.

Bond, T.C., Doherty, S.J., Fahey, D.W., Forster, P.M., Berntsen, T., DeAngelo, B.J., Flanner, M.G., Ghan, S., Kaercher, B., Koch, D., et al., 2013. Bounding the role of black carbon in the climate system: a scientific assessment. J. Geophys. Res. Atmos. 118, 5380–5552.

Brown, S.G., Lee, T., Roberts, P.T., Collett Jr., J.L., 2013. Variations in the OM/OC ratio of urban organic aerosol next to a major roadway. J. Air Waste Manag. 63, 1422–1433.

Brown, R.J.C., Beccacesi, S., Butterfield, D.M., Quincey, P.G., Harris, P.M., Maggos, T., Panteliadis, P., John, A., Jedynska, A., Kuhlbusch, T.A.J., Putaud, J.-P., Karanasiou, A., 2017. Standardisation of a European measurement method for organic carbon and elemental carbon in ambient air: results of the field trial campaign and the determination of a measurement uncertainty and working range. Environmental Science: Processes and Impacts 19, 1249–1259.

Brown, S., Minor, H., O'Brien, T., Hameed, Y., Feenstra, B., Kuebler, D., Wetherell, W., Day, R., Tun, R., Landis, E., Rice, J., 2019. Review of sunset OC/EC instrument measurements during the EPA's sunset carbon evaluation project. Atmosphere 10, 287. https://doi.org/10.3390/atmos10050287.

Budisulistiorini, S.H., Canagaratna, M.R., Croteau, P.L., Baumann, K., Edgerton, E.S., Kollman, M.S., Ng, N.L., Verma, V., Shaw, S.L., Knipping, E.M., et al., 2014. Intercomparison of an Aerosol Chemical Speciation Monitor (ACSM) with ambient fine aerosol measurements in downtown Atlanta, Georgia. Atmos. Meas. Tech. 7, 1929–1941.

Carslaw, D.C., Ropkins, K., 2012. Openair — an R package for air quality data analysis. Environ. Model Softw. 27–28 (0), 52–61 ISSN 1364-8152. https://doi.org/10.1016/j.envsoft.2011.09.008.

Cavalli, F., Viana, M., Yttri, K.E., Genberg, J., Putaud, J.-P., 2010. Toward a standardized thermal-optical protocol for measuring atmospheric organic and elemental carbon: the EUSAAR protocol. Atmos. Meas. Tech. 3, 79–89.

Cavalli, F., Alastuey, A., Areskoug, H., Ceburnis, D., Cech, J., Genberg, J., Harrison, R.M., Jaffrezo, J.L., Kiss, G., Laj, P., Mihalopoulos, N., Perez, N., Quincey, P., Schwarz, J., Sellegri, K., Spindler, G., Swietlicki, E., Theodosi, C., Yttri, K.E., Aas, W., Putaud, J.P., 2016. A European aerosol phenomenology -4: harmonized concentrations of carbonaceous aerosol at 10 regional background sites across Europe. Atmos. Environ. 144, 133–145.

Cesari, D., Merico, E., Dinoi, A., Marinoni, A., Bonasoni, P., Contini, D., 2018. Seasonal variability of carbonaceous aerosols in an urban background area in Southern Italy. Atmos. Res. 200, 97–108.

Chang, Y., Deng, C., Cao, F., Cao, C., Zou, Z., Liu, S., Lee, X., Li, J., Zhang, G., Zhang, Y., 2017. Assessment of carbonaceous aerosols in Shanghai, China – part 1: long-term evolution, seasonal variations, and meteorological effects. Atmos. Chem. Phys. 17, 9945–9964. https://doi.org/10.5194/acp-17-9945-2017.

Chow, J.C., Watson, J.G., Pritchett, L.C., Pierson, W.R., Frazier, C.A., Purcell, R.G., 1993. The DRI thermal/optical reflectance carbon analysis system: description, evaluation and applications in US air quality studies. Atmos. Environ. 27, 1185–1201.

Chow, J.C., Watson, J.G., Crow, D., Lowenthal, D.H., Merrifield, T., 2001. Comparison of IMPROVE and NIOSH carbon measurements. Aerosol Sci. Technol. 34 (1), 23–34.

Contini, D., Vecchi, R., Viana, M., 2018. Carbonaceous aerosols in the atmosphere. Atmosphere 9, 181.

Crenn, V., Chakraborty, A., Fronval, I., Petitprez, D., Riffault, V., 2018. Fine particles sampled at an urban background site and an industrialized coastal site in Northern France—part 2: comparison of offline and online analyses for carbonaceous aerosols. Aerosol Sci. Technol. 52 (3), 287–299. https://doi.org/10.1080/02786826.2017.1403008.

Docherty, K.S., Aiken, A.C., Human, J.A., Ulbrich, I.M., DeCarlo, P.F., Sueper, D., Worsnop, D.R., Snyder, D.C., Peltier, R.E., Weber, R.J., et al., 2011. The 2005 study of organic aerosols at Riverside (SOAR-1): instrumental intercomparisons and fine particle composition. Atmos. Chem. Phys. 11, 12387–12420.

European Committee for Standardisation, 2017. EN 16909:2017, Ambient Air – Measurement of Elemental Carbon (EC) and Organic Carbon (OC) Collected on Filters. CEN, Brussels.

Fung, K.K., Chow, J.C., Watson, J.G., 2002. Evaluation of OC/EC speciation by thermal manganese dioxide oxidation and the IMPROVE method. J. Air Waste Manage. Assoc. 52 (11), 1333–1341.

Fuzzi, S., Andreae, M.O., Huebert, B.J., Kulmala, M., Bond, T.C., Boy, M., Doherty, S.J., Guenther, A., Kanakidou, M., Kawamura, K., Kerminen, V.-M., Lohmann, U., Russell, L.M., Pöschl, U., 2006. Critical assessment of the current state of scientific knowledge, terminology, and research needs concerning the role of organic aerosols in the atmosphere, climate, and global change. Atmos. Chem. Phys. 6, 2017–2038. https://doi.org/10.5194/acp-6-2017-2006.

Giannoni, M., Calzolai, G., Chiari, M., Cincinelli, A., Lucarelli, F., Martellini, T., Nava, S., 2016. A comparison between thermal-optical transmittance elemental carbon measured by different protocols in PM2.5 samples. Sci. Total Environ. 571, 195–205.

Healy, R.M., Sofowote, U., Su, Y., Debosz, J., Noble, M., Jeong, C.-H., Wang, J.M., Hilker, N., Evans, G.J., Doerksen, G., 2017. Ambient measurements and source apportionment of fossil fuel and biomass burning black carbon in Ontario. Atmos. Environ. 161, 34–47.

Janssen, N.A.H., Hoek, G., Simic-Lawson, M., Fischer, P., van Bree, L., ten Brink, H., Keuken, M., Atkinson, R.W., Anderson, H.R., Brunekreef, B., et al., 2011. Black carbon as an additional indicator of the adverse health effects of airborne particles compared with PM10 and PM2.5. Environ. Health Perspect. 119, 1691–1699.

Jeong, C.H., Hopke, P.K., Kim, E., Lee, D.W., 2004. The comparison between thermal optical transmittance elemental carbon and Aethalometer black carbon measured at multiple monitoring sites. Atmos. Environ. 38, 5193–5204.

Jimenez, J.L., Canagaratna, M.R., Donahue, N.M., Prevot, A.S.H., Zhang, Q., Kroll, J.H., DeCarlo, P.F., Allan, J.D., Coe, H., Ng, N.L., Aiken, A.C., Docherty, K.S., Ulbrich, I.M., Grieshop, A.P., Robinson, A.L., Duplissy, J., Smith, J.D., Wilson, K.R., Lanz, V.A., Hueglin, C., Sun, Y.L., Tian, J., Laaksonen, A., Raatikainen, T., Rautiainen, J., Vaattovaara, P., Ehn, M., Kulmala, M., Tomlinson, J.M., Collins, D.R., Cubison, M.J., Dunlea, E.J., Human, J. a, Onasch, T.B., Alfarra, M.R., Williams, P.I., Bower, K., Kondo, Y., Schneider, J., Drewnick, F., Borrmann, S., Weimer, S., Demerjian, K., Salcedo, D., Cottrell, L., Grin, R., Takami, A., Miyoshi, T., Hatakeyama, S., Shimono, A., Sun, J.Y., Zhang, Y.M., Dzepina, K., Kimmel, J.R., Sueper, D., Jayne, J.T., Herndon, S.C., Trimborn, A.M., Williams, L.R., Wood, E.C., Middlebrook, A.M., Kolb, C.E., Baltensperger, U., Worsnop, D.R., 2009. Evolution of organic aerosols in the atmosphere. Science 326, 1525–1529.

Jung, J., Kim, Y.J., Lee, K.Y., Kawamura, K., Hu, M., Kondo, Y., 2011. The effects of accumulated refractory particles and the peak inert mode temperature on semicontinuous organic and elemental carbon measurements during CARE Beijing 2006 campaign. Atmos. Environ. 45, 7192–7200.

Kanakidou, M., Seinfeld, J.H., Pandis, S.N., Barnes, I., Dentener, F.J., Facchini, M.C., Van Dingenen, R., Ervens, B., Nenes, A., Nielsen, C.J., et al., 2005. Organic aerosol and global climate modelling: a review. Atmos. Chem. Phys. 5, 1053–1123.

Kanaya, Y., Komazaki, Y., Pochanart, P., Liu, Y., Akimoto, H., Gao, J., Wang, T., Wang, Z., 2008. Mass concentrations of black carbon measured by four instruments in the middle of central East China in June 2006. Atmos. Chem. Phys. 8, 7637–7649.

Karanasiou, A., Minguillón, M.C., Viana, M., Alastuey, A., Putaud, J.P., Maenhaut, W., Panteliadis, P., Mocnik, G., Favez, O., Kuhlbusch, T.A.J., 2015. Thermal-optical analysis for the measurement of elemental carbon (EC) and organic carbon(OC) in ambient air a literature review. Atmos. Meas. Tech. Discuss. 8, 9649–9712. https://doi.org/10.5194/amtd-8-9649-2015.

Lee, B.P., Li, Y.J., Yu, J.Z., Louie, P.K.K., Chan, C.K., 2013. Physical and chemical characterization of ambient aerosol by HR-ToF-AMS at a suburban site in Hong Kong during springtime 2011. J. Geophys. Res. Atmos. 118, 8625–8639.

Malaguti, A., Mircea, M., LaTorretta, T.M.G., Telloli, C., Petralia, E., Stracquadanio, M., Berico, M., 2015. Comparison of online and offline methods for measuring fine secondary inorganic ions and carbonaceous aerosols in the central mediterranean area. Aerosol Air Qual. Res. 15 (7), 2641–2653.

Massling, A., Nielsen, I.E., Kristensen, D., Christensen, J.H., Sørensen, L.L., Jensen, B., Nguyen, Q.T., Nøjgaard, Q.T., Glasius, M., Skov, H., 2015. Atmospheric black carbon and sulfate concentrations in Northeast Greenland. Atmos. Chem. Phys. 15, 9681–9692.

Minguillón, M.C., Ripoll, A., Pérez, N., Prévôt, A.S.H., Canonaco, F., Querol, X., Alastuey, A., 2015. Chemical characterization of submicron regional background aerosols in the western Mediterranean using an aerosol chemical speciation monitor. Atmos. Chem. Phys. 15, 6379–6391. https://doi.org/10.5194/acp-15-6379-2015.

Minguillón, M.C., Pérez, N., Marchand, N., Bertrand, A., Temime-Roussel, B., Agrios, K., Szidat, S., van Drooge, B., Sylvestre, A., Alastuey, A., Reche, C., Ripoll, A., Marco, E., Grimalt, J.O., Querol, X., 2016. Secondary organic aerosol origin in an urban environment: influence of biogenic and fuel combustion precursors. Faraday Discuss. 189, 337–359.

Pandolfi, M., Querol, X., Alastuey, A., Jimenez, J.L., Jorba, O., Day, D., Ortega, A., Cubison, M.J., Comerón, A., Sicard, M., Mohr, C., Prévôt, A.S.H., Minguillón, M.C., Pey, J., Baldasano, J.M., Burkhart, J.F., Seco, R., Peñuelas, J., van Drooge, B.L., Artiñano, B., Di Marco, C., Nemitz, E., Schallhart, S., Metzger, A., Hansel, A., Lorente, J., Ng, S., Jayne, J., Szidat, S., 2014. Effects of sources and meteorology on particulate matter in the Western Mediterranean Basin: an overview of the DAURE campaign. J. Geophys. Res. Atmos. https://doi.org/10.1002/2013JD021079.

Panteliadis, P., Hafkenscheid, T., Cary, B., Diapouli, E., Fischer, A., Favez, O., Quincey, P., Viana, M., Hitzenberger, R., Vecchi, R., Saraga, D., Sciare, J., Jaffrezo, J.L., John, A., Schwarz, J., Giannoni, M., Novak, J., Karanasiou, A., Fermo, P., Maenhaut, W., 2015. ECOC comparison exercise with identical thermal protocols after temperature offset

correction – instrument diagnostics by in-depth evaluation of operational parameters. Atmos. Meas. Tech. 8, 779–792. https://doi.org/10.5194/amt-8-779-2015.

Park, K., Chow, J.C., Watson, J.G., Trimble, D.L., Doraiswamy, P., Arnott, W.P., Stroud, K.R., Bowers, K., Bode, R., Petzold, A., Hansen, A.D., 2006. Comparison of continuous and filter-based carbon measurements at the Fresno supersite. J. Air Waste Manage. Assoc. 56 (4), 474–491.

Petzold, A., Ogren, J.A., Fiebig, M., Laj, P., Li, S.-M., Baltensperger, U., Holzer-Popp, T., Kinne, S., Pappalardo, G., Sugimoto, N., Wehrli, C., Wiedensohler, A., Zhang, X.-Y., 2013. Recommendations for reporting "black carbon" measurements. Atmos. Chem. Phys. 13, 8365–8379. https://doi.org/10.5194/acp-13-8365-2013.

Pey, J., Querol, X., Alastuey, A., Forastiere, F., Stafoggia, M., 2013. African dust outbreaks over the Mediterranean Basin during 2001-2011: PM10 concentrations, phenomenology and trends, and its relation with synoptic and mesoscale meteorology Atmos. Chem. Phys. 13, 1395–1410.

Putaud, J.P., Van Dingenen, R., Alastuey, A., Bauer, H., Birmili, W., Cyrys, J., Flentje, H., Fuzzi, S., Gehrig, R., Hansson, H.C., et al., 2010. A European aerosol phenomenology-3: physical and chemical characteristics of particulate matter from 60 rural, urban, and kerbside sites across Europe. Atmos. Environ. 44, 1308–1320.

Querol, X., Alastuey, A., Rodríguez, S., Plana, F., Mantilla, E., Ruiz, C.R., 2001. Monitoring of PM10 and PM2.5 around primary particulate anthropogenic emission sources. Atmos. Environ. 35, 845–858.

Querol, X., Alastuey, A., Viana, M., Moreno, T., Reche, C., Minguillón, M.C., et al., 2013. Variability of carbonaceous aerosols in remote, rural, urban and industrial environments in Spain: implications for air quality policy. Atmos. Chem. Phys. 13 (13), 6185–6206.

Querol, X., Tobías, A., Pérez, N., Karanasiou, A., Amato, F., Stafoggia, M., García-Pando, C.P., Ginoux, P., Forastiere, F., Gumy, S., et al., 2019. Monitoring the impact of desert dust outbreaks for air quality for health studies. Environ. Int. 130, 104867.

Rattigan, O.V., Felton, H.D., Bae, M.-S., Schwab, J.J., Demerjian, K.L., 2010. Multi-year hourly PM2.5 carbon measurements in New York: diurnal, day of week and seasonal patterns. Atmos. Environ. 44, 2043–2053.

Reche, C., Querol, X., Alastuey, A., Viana, M., Pey, J., Moreno, T., Rodriguez, S., González Ramos, Y., Fernandez-Camacho, R., Verdona, Ana M., de la Rosa, J.D., Dall'osto, M., Prevot, A., Hueglin, C., Harrison, R., Quincey, P., 2011. New considerations for PM, black carbon and particle number concentration for air quality monitoring across different European cities. Atmos. Chem. Phys. 11, 6207–6227. https://doi.org/10.5194/acp-11-6207-2011.

Reisinger, P., Wonaschütz, A., Hitzenberger, R., Petzold, A., Bauer, H., Jankowski, N., Puxbaum, H., Chi, X., Maenhaut, W., 2008. Intercomparison of measurement techniques for black or elemental carbon under urban background conditions in wintertime: influence of biomass combustion. Environ. Sci. Technol. 42, 884–889.

Sandrini, S., Fuzzi, S., Piazzalunga, A., Prati, P., Bonasoni, P., Cavalli, F., Bove, M.C., Calvello, M., Cappelletti, D., Colombi, C., et al., 2014. Spatial and seasonal variability of carbonaceous aerosol across Italy. Atmos. Environ. 99, 587–598.

Snyder, D.C., Schauer, J., 2007. An inter-comparison of two black carbon aerosol instruments and a Semi-Continuous elemental carbon instrument in the urban environment. Aerosol Sci. Technol. 41, 463–474.

Takegawa, N., Miyazaki, Y., Kondo, Y., Komazaki, Y., Miyakawa, T., Jimenez, J.L., Jayne, J.T., Worsnop, D.R., Allan, J.D., Weber, R.J., 2005. Characterization of an Aerodyne Aerosol Mass Spectrometer (AMS): intercomparison with other aerosol instruments. Aerosol Sci. Technol. 39, 760–770.

Titos, G., Ealo, M., Pandolfi, M., Pérez, N., Sola, Y., Sicard, M., Comerón, A., Querol, X., Alastuey, A., 2017. Spatiotemporal evolution of a severe winter dust event in the western Mediterranean: aerosol optical and physical properties. J. Geophys. Res. Atmos. 122, 4052–4069. https://doi.org/10.1002/2016JD026252.

Turpin, B.J., Huntzicker, J.J., 1991. Secondary formation of organic aerosol in the Los Angeles basin: a descriptive analysis of organic and elemental carbon concentrations. Atmos. Environ. 25, 207–215. https://doi.org/10.1016/0960-1686(91)90291-E.

Venkatachari, Prasanna, Zhou, Liming, Hopke, Philip K., Schwab, James J., Demerjian, Kenneth L., Weimer, Silke, Hogrefe, Olga, Felton, Dirk, Rattigan, Oliver, 2006. An intercomparison of measurement methods for carbonaceous aerosol in the ambient air in NewYork City. Aerosol Sci. Technol. 40 (10), 788–795. https://doi.org/10.1080/02786820500380289.

Viana, M., Chi, X., Maenhaut, W., Cafmeyer, J., Querol, X., Alastuey, A., Mikuška, P., Večeřa, Z., 2006. Influence of sampling artefacts on measured PM, OC, and EC levels in carbonaceous aerosols in an urban area. Aerosol Sci. Technol. 40, 107–117. https://doi.org/10.1080/02786820500484388.

Vodička, Petr, Schwarz, Jaroslav, Cusack, Michael, Ždímal, Vladimír, 2015. Detailed comparison of OC/EC aerosol at an urban and a rural Czech background site during summer and winter. Sci. Total Environ. 518-519, 424–433. https://doi.org/10.1016/j.scitotenv.2015.03.029.

Xu, W., Lambe, A., Silva, P., Hu, W., Onasch, T., Williams, L., Croteau, P., Zhang, X., Renbaum-Wolff, L., Fortner, E., Jimenez, J.L., Jayne, J., Worsnop, D., Canagaratna, M., 2018. Laboratory evaluation of species-dependent relative ionization efficiencies in the aerodyne aerosol mass spectrometer. Aerosol Sci. Technol. 52 (6), 626–641. https://doi.org/10.1080/02786826.2018.1439570.

Zanatta, M., Gysel, M., Bukowiecki, N., Muller, T., Weingartner, E., Areskoug, H., Fiebig, M., ... Laj, P., 2016. A European aerosol phenomenology-5: climatology of black carbon optical properties at 9 regional background sites across Europe. Atmos. Environ. 145, 346–364. https://doi.org/10.1016/j.atmosenv.2016.09.035.

Zíková, Naděžda, Vodička, Petr, Ludwig, Wolfgang, Hitzenberger, Regina, Schwarz, Jaroslav, 2016. On the use of the field sunset semi-continuous analyzer to measure equivalent black carbon concentrations. Aerosol Sci. Technol. 50 (3), 284–296. https://doi.org/10.1080/02786826.2016.1146819.